Journal of Photochemistry and Photobiology A: Chemistry 221 (2011) 64–70

Contents lists available at ScienceDirect

Journal of Photochemistry and Photobiology A: Chemistry

journal homepage: www.elsevier.com/locate/jphotochem

Lipid vesicles as model membranes in photocatalytic disinfection studies

O.K. Dalrymple, W. Isaacs, E. Stefanakos, M.A. Trotz, D.Y. Goswami*

Clean Energy Research Center, University of South Florida, Tampa, FL 33620, USA

ARTICLE INFO

Article history:
Received 2 November 2010
Received in revised form 12 April 2011
Accepted 24 April 2011
Available online 30 April 2011

Keywords:
Hydroperoxide
Malondialdehyde
Peroxidation
Phosphatidylethanolamine
TBARS
Titanium dioxide

ABSTRACT

The potential use of solar-powered photocatalytic disinfection water systems is an attractive concept and has generated much research over the last two decades. Photocatalytic inactivation of a wide range of water pathogens has shown promise to provide an effective alternative to traditional disinfection methods. However, in order for photocatalysis to be effectively used as a water disinfection process, its inactivation kinetics must be well established. Recent literature points to the peroxidation of phospholipid membranes as the main mechanism for photocatalytic inactivation of bacteria. To test the peroxidation hypothesis, researchers utilized free lipids, particularly lipids with the ethanolamine polar group which is dominant in the cell membrane of *Escherichia coli*. Although these experiments yielded useful information about byproducts, they did not provide information on the kinetics of lipid peroxidation in cells exposed to photocatalytic treatment.

In this work, lipid vesicles were prepared with a mixture of natural *E. coli* phospholipids and appropriately sized to be comparable to real cells. The vesicles and *E. coli* cells were photocatalytically treated in a test tube batch reactor using TiO_2 (Degussa P25) and UVA lamps. The rate of phospholipid membrane degradation was determined by measuring the production of malondialdehyde (MDA) and lipid hydroperoxide (LOOH), byproducts of lipid peroxidation. Thiobarbituric Acid Reactive Species (TBARS) and Ferrous Oxidation of Xylenol (FOX) assays were used to assess each byproduct respectively. The fatty acid content of *E. coli* cells was also modified by adding oleic (C18:1 n-9) and α-linolenic (C18:3 n-3) acids to the growth media. Byproduct formation and oxidation kinetics were compared for all experiments. The results show that the oxidation kinetics of lipid vesicles closely matched the oxidation of *E. coli* cells in photocatalytic systems proving that the vesicles are useful model systems to study the interaction of cell membranes with TiO_2. However, differences in monosaturated fatty acids in *E. coli* did not appear to affect the overall disinfection kinetics. While these findings further validate membrane peroxidation as an important process in the mechanism of photocatalytic disinfection, they suggest that overall inactivation results from a far more complex collection of processes.

1. Introduction

Over the past decade the mechanism of photocatalytic disinfection has been heavily debated among researchers. Increasing evidence suggests that the oxidation of cell membrane lipids plays an important role in the photocatalytic inactivation of bacterial pathogens in water [1–5]. The general hypothesis is that the unsaturated fatty acids, mainly polyunsaturated fatty acids, present in the phospholipid membranes are very sensitive to oxidation by radical species, particularly the hydroxyl radical. The repeating arrangement of lipids in the membrane allows cell injury to occur at sites relatively distant from the initiation source due to radical-induced chain reactions (Fig. 1).

During photocatalysis hydroxyl radicals are generated on the surface of a solid semiconductor catalyst, such as titanium dioxide (TiO_2), when exposed to light of the appropriate wavelength [6]. The hydroxyl radical is known to oxidize all macromolecules found in cells including proteins [7,8], polysaccharides [9], lipids [10–12], and nucleic acids [13,14]. However, the disinfection process is mainly characterized by an interaction between the cell membrane and the photocatalyst [15]. The phospholipid components of the cell are localized in the cell membrane. TiO_2 is capable of initiating an irreversible oxidation of the fatty acids present in the membrane of the pathogen when hydroxyl radicals extract H-atoms from unsaturated lipids. The initiation process is followed by a propagation cycle in which the newly formed lipid radical reacts with oxygen to produce a lipid peroxyl radical. The propagation cycle continues as the lipid peroxyl radical reacts with a nearby unsaturated lipid producing a new lipid radical and a lipid hydroperoxide (LOOH). The process is terminated when two radicals react forming a non-radical species. The lipid hydroper-

* Corresponding author. Tel.: +1 8139740956; fax: +1 8139746438.
E-mail addresses: odalrymp@mail.usf.edu (O.K. Dalrymple), goswami@usf.edu (D.Y. Goswami).

1010-6030/$ – see front matter © 2011 Elsevier B.V. All rights reserved.
doi:10.1016/j.jphotochem.2011.04.025

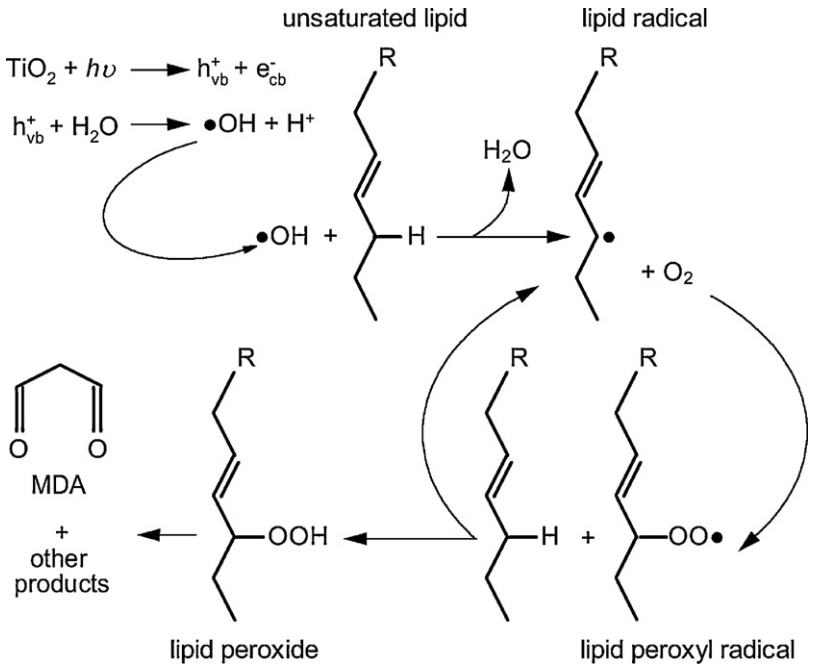

Fig. 1. Schematic of radical-induced lipid peroxidation.

oxide can further be oxidized by lipid radicals to form aldehydes, especially MDA. The latter is often used as a biomarker for lipid peroxidation in cells. The process of lipid peroxidation leads to the destruction of the cell membrane, disrupting its functions and eventually leading to cell inactivation [10,16].

The lipid composition of bacterial membranes depends very much on the species and even on the culture conditions and stage in the growth cycle. Membrane fractions usually contain 10–30% lipid. In Gram-positive bacteria phosphatidylglycerol (PG) is present, but phosphatidylethanolamine (PE) is more common in Gram-negative species. Phosphatidylethanolamine can form 75% of the total phospholipids in *E. coli*. The other lipids are PG and cardiolipin; the proportion of each depends on the growth phase [17,18]. Phospholipids have a fatty acid tail, which have the potential to serve as initiation sources for membrane peroxidation. This is particularly true for polyunsaturated fatty acids, even though they are often present in smaller proportions than monosaturated fatty acids. In *E. coli* unsaturated fatty acids can account for as much as 50% of all fatty acids, and generally include palmitoleic acid (C16:1 n-7) and *cis*-vaccenic (C18:1 n-7) [17,19–22]. It is therefore suspected that the kinetics of peroxidation of the cell membrane may be affected by the fatty acid content of the cell, mainly the unsaturated species.

In previous studies of photocatalytic disinfection, lipid peroxidation was confirmed by comparing MDA production during photocatalytic oxidation of PE and *E. coli* cells [1,4]. However, in these studies PE was used in a dissolved form in a homogenous solution. While this approach yielded useful information about byproduct formation, it does not offer much information on the kinetics of cell membrane oxidation because chain reactions in a compartmentalized membrane system can follow very different kinetics and mechanisms from those observed in homogeneous solutions [23]. In addition, unlike other phospholipids which spontaneously form lamellar phases in aqueous media, pure PE solutions or mixtures enriched in PE are notable for being unstable and adopt a hexagonal phase [24,25]. They often require a stabilizing agent to maintain a bilayer structure similar to biological membranes.

The current study goes further to establish lipid peroxidation in cells during photocatalysis by using lipid vesicles as model *E. coli* membranes. Lipid vesicles of PE were prepared with the addition of PG, which served as a stabilizing agent, but also represented a more realistic and natural *E. coli* membrane. The vesicles were also sized to be comparable to real cells to mimic the colloidal nature of the solution. In addition, the effect of unsaturated fatty acid enrichment in *E. coli* on peroxidation kinetics was also tested. Enrichment was achieved by supplementing the growth media with oleic and α-linolenic acids and validated by fatty acid methyl ester (FAME) analysis. The cells and vesicles were then exposed to illumination with TiO_2 and the evolution of MDA and LOOH was measured during the experiments to assess membrane peroxidation.

2. Materials and methods

2.1. Cell culture

E. coli ATCC 25922 was grown aerobically in 100 mL of Luria broth at 37 °C in an incubator shaker (250 rpm) for 6 h (to log phase). The cells were harvested from the broth by centrifugation at 1380 × *g* for 10 min in a 15-mL polypropylene centrifuge tube. The cell pellet was washed and re-suspended in sterile deionized water (resistivity >16 Mohm-cm). This process was performed twice to ensure that most of the broth solution was removed. The turbidity of the suspension was measured at 550 nm with a DR/2000 spectrophotometer (Hach Company). The cell suspension was diluted to the required final concentration for all experiments based on a standard curve that correlated turbidity with cell concentration (CFU mL^{-1}). Lipid modification of the cells was achieved by supplementing the Luria broth base with 32 μM of oleic (C18:1 n-9) and α-linolenic (C18:3 n-3) acids obtained from MP Biomedicals (Solon, OH).

2.2. Fatty acid analysis

At least 20 mg of cells was harvested and twice pelletized by centrifugation at 1380 × *g* for 15 min in a 15-mL tube after successive washing of the cells with sterile deionized water. The cell pellets were sent to Microbial ID (Newark, DE) for fatty acid methyl ester (FAME) analysis. The general steps in a FAME analysis included extraction of the fatty acids by a procedure which consisted of

saponification in dilute sodium hydroxide/methanol solution, followed by derivatization with dilute hydrochloric acid/methanol solution to give respective methyl esters. The methyl esters are then extracted from the aqueous phase by the use of an organic solvent and the resulting extract was analyzed by gas chromatography (GC).

2.3. Lipid vesicle preparation and characterization

E. coli PE and PG were obtained from Avanti Polar Lipids (Alabaster, AL) dissolved in chloroform with a concentration of 5 mg mL^{-1} each. To prepare a 1:1 molar ratio, 2 mL of PE was mixed with 1.74 mL of PG. Higher ratios of PE to PG were initially used, but the stability of the liposomes was not consistent. The PE–PG solution was transferred to a clean and dry 100-mL round bottom flask and continuously rotated by hand in a water bath at 60 °C until the solvent evaporated and a uniform thin lipid film was formed on the surface of the flask. A gentle stream of N_2 gas was passed over the film to remove solvent vapor. The flask was left overnight in a chemical hood to allow complete evaporation of all the chloroform. Hydration was performed with 5 mL of 0.01 M of phosphate buffer saline (PBS) solution by continuously rotating the flask in the water bath maintained at 60 °C until all the film was completely dissolved (smooth milky white appearance). The size reduction step was done using a mini extruder from Avanti Polar Lipids (Alabaster, AL). The extruder was maintained at 60 °C and extrusion done 12 times through the syringes using a 0.8-μm polycarbonate membrane. The size distribution of the lipid vesicles was determined by photon correlation spectroscopy using Malvern Zetasizer Nano series device. A drop of the PE–PG solution was placed on a Formvar carbon film with 150 square mesh copper grids and visually examined with a FEI Morgagni 268 transmission electron microscope (TEM) after staining with 0.5% uranyl acetate in water. The TEM was operated at 60 kV and an Olympus Soft Imaging MegaView III camera was used to collect images.

2.4. Photocatalytic reaction

Degussa P25 TiO_2 was used as the catalyst for experiments. The formulation of this catalyst has been published extensively as containing 75% anatase and 25% rutile, with an average surface area of 50 m^2 g^{-1}. A stock solution of 10 mg mL^{-1} was prepared by vigorously mixing the catalyst with deionized water, autoclaving, and storing the suspension at room temperature. The final catalyst concentration used was 1 mg mL^{-1}. Experiments were conducted in 30-mL borosilicate test tubes, which were placed between two 9-W UVA lamps (PL9W/08, Philips). The lamps have a spectral maximum at 365 nm. The solution was continuously stirred on magnetic stir plates. The pH was initially monitored, but since it did not change significantly (7.5 ± 0.05), only the initial pH of subsequent experiments was measured. Three sets of control experiments were conducted; TiO_2 only, UV only, and standing water without catalyst and light. All experiments were conducted in triplicates. The light intensity was determined by azoxybenzene actinometry [26] to be $4.37 \times 10^{-2} \pm 5.19 \times 10^{-3}$ mE L^{-1} s^{-1}.

2.5. Cell viability assay

The concentration of cells in suspension was determined by plating on Tryptic soy agar. Aliquots of 100 μL were taken from the reactor at various time intervals during the course of the experiments. Each sample was serially diluted and specific dilutions plated in triplicates. The plates were incubated at 37 °C for 24 h and the colonies that appeared were counted.

2.6. MDA assay

A TBARS assay kit was obtained from Northwest Life Science Specialties (Vancouver, WA) and used to measure MDA in the samples. Aliquots of 250 μL sample solution were added to a microcentrifuge vial containing 10 μL butylated hydroxytoluene (BHT). 250 μL of the acid reagent was added and the mixture was centrifuged at 11,000 × *g* for 35 min and then for an additional 20 min to remove solids. The supernatant was transferred to new vials and 250 μL of TBA reagent was added. The mixture was vigorously shaken on a vortex for 5 counts and then incubated in a water bath at 60 °C for 1 h. After incubation, the solution was centrifuged at 10,000 × *g* for 3 min and absorbance of the supernatant was recorded from 400 to 700 nm on an Ocean Optic USB2000 spectrometer using the OOIBase 32 software and DH-2000-BAL UV–VIS light source. Derivative spectroscopy analysis was performed on the absorbance spectra to negate the effects of non-linear baselines and enhance the spectral signals. The second derivative was selected and the absorbance evaluated at 511 nm.

2.7. LOOH assay

This kit was also obtained from Northwest Life Science Specialties (Vancouver, WA). The method is based on the fact that a hydroperoxide present in solution oxidizes ferrous iron (Fe^{2+}) to ferric iron (Fe^{3+}) under acidic conditions [27,28]. The resulting ferric iron was detected using xylenol orange, which forms a Fe^{3+}–xylenol orange complex. The complex was measured on a spectrophotometer at 560 nm. The manufacturer's assay protocol was followed precisely, except for an additional final centrifugation step to remove solids in the samples.

3. Results and discussion

3.1. Fatty acid profiles

The fatty acid profile of the unmodified *E. coli* was a close match to published profiles of the organisms; see for example [19,20,29]. The predominant fatty acid was the saturated 16-carbon (palmitic acid). In the control organism, palmitoleic (C16:1 n-7) and *cis*-vaccenic (C18:1 n-7) acids were present in equal proportions and accounted for most of the monounsaturated content. The total polyunsaturated fatty acid content was below 0.5%. Monosaturated fatty acids in the organism increased in accordance with the specific supplement. Organisms supplemented with oleic acid (C18:1 n-9) had an enrichment of this fatty acid in their membrane, even though it was not detected in the control population. The enrichment was accompanied by a reduction in the positional isomer of oleic acid, *cis*-vaccenic acid.

The addition of α-linolenic acid (C18:3 n-3) had a pronounced effect on the fatty acid distribution. The presence of α-linolenic was not detected in the samples indicating that the supplemental fatty acid was converted by the organisms to other, less unsaturated fatty acids. There were significant changes particularly in content of *cis*-vaccenic acid and the appearance of a small fraction of C18:2 in the organism.

3.2. Lipid vesicle composition and size distribution

The average diameter of the lipid vesicles was approximately 0.5 μm (Fig. 2). Even though the vesicles are not rod-shaped like *E. coli*, the results correspond well to the published data on the size of *E. coli* cells, which measure on average 0.5 μm by 1 μm [30]. The size and shape of the vesicles were confirmed with TEM images as shown in Fig. 3. The size distribution of the vesicles is important

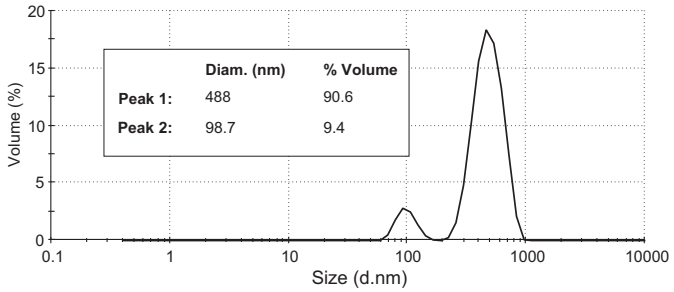

Fig. 2. Size distribution by volume based on photon correlation spectroscopy of the lipids vesicles in 1× PBS solution (molar ratio 1:1 PE to PG).

to establish the precise kinetic behavior of the system. The interaction of the particles (photocatalyst and cell) is based on particle size. Particles of similar sizes are more likely to be described by a collision model, whereas smaller particles are expected to adsorb or attach to sites on larger ones [15].

The very distinct darkened outline on the features in Fig. 3 indicates that these were most likely multilamellar vesicles. Due to the nature of the TEM sample preparation, many of the vesicles seen in the figure were the very large vesicles which settled out unto the TEM grid. The fatty acid composition of the vesicles was estimated from the manufacturer's data and is shown in Table 1. The predominant unsaturated fatty acid was *cis*-vaccenic acid (C18:1 n-7) in PE and oleic acid (C18:1 n-9) in PG.

3.3. MDA production during photocatalytic experiments

Even though the MDA test has some limitations, the evolution of MDA in all the samples was very similar and consistent between experiments. The monotonic accumulation of MDA was observed during the first 20–30 min of the photocatalytic experiments for both unmodified *E. coli* cells and lipid vesicles. Thereafter, a steady decrease in concentration was recorded (Fig. 4). There was a prolonged increase in MDA for the cells modified with linolenic acid. The overall trend for MDA release during photocatalysis was first observed by Maness et al. [1] for the disinfection of *E. coli* cells under similar conditions. The trend appears to be consistent with the peroxidation of membrane lipids followed by the degradation of MDA (either naturally or photocatalytically). More MDA was produced in the vesicles because they were composed only of fatty acids, whereas cells have their fatty acids distributed in the membrane with other biological structures such as proteins.

A common criticism of the TBA assay is that MDA is artefactually formed during the harsh processing conditions of the test [31–35]. However, the use of BHT antioxidant in the test serves to eliminate or reduce the production of MDA during the processing of the sample [32]. In addition, the conditions of these tests were much milder compared to the more traditional TBA tests which utilize boiling temperatures to facilitate the reaction with MDA. The most convincing evidence of all is the fact that no measurable MDA concentrations were detected in any of the control experiments (data not shown), leading to the conclusion that the observed trend resulted from treating the cells and vesicles photocatalytically.

The TBA test is the most frequently used method to detect lipid peroxidation, but it has also been criticized for its non-specificity, particularly in complex biological systems. However, it has proven useful in well defined systems such as the oxidation of lipid vesicles [36,37]. Hence, when the time characteristic for MDA evolution during oxidation of the model membranes is compared to real cells, there is strong evidence that the trend observed in cells resulted from membrane peroxidation.

Table 1
Percent distribution of major fatty acids.

Fatty acids	Unmodified cells[a]	Fatty acid supplement		Lipid vesicles[b]
		C18:1 n-9	C18:3 n-3	
Saturated				
C14	8.5	7.6	7.4	1.8
C15	1.9	1.6	1.5	8.5
C16	34.8	31.9	32.6	28.8
C17	2.1	1.6	2.1	10.9
C18	0.6	0.3	1.0	0.0
Monounsaturated				
C16:1n-7	12.5	5.2	9.5	7.1
C18:1n-7	12.6	6.7	17.3	17.1
C18:1n-9	0.0	22.2	2.8	4.5
Polyunsaturated				
C18:2n-6	0.4	0.0	2.7	0.0
Cyclopropane				
C17	11.1	6.3	9.0	14.5
C19	1.3	1.9	1.2	4.0
Total saturated	73.2	63.6	66.6	68.5
Total unsaturated	26.2	35.9	32.8	28.7
Unsaturated/saturated	0.4	0.6	0.5	0.4

[a] *E. coli* cells grown in Luria broth and harvested at 6 h. Only major fatty acids are shown. Total fatty acids include all fatty acids detected in analysis. See supplemental information.
[b] Fatty acid spectra obtained from manufacturer.

3.4. Effect of supplemental fatty acid on MDA production in cells

For the cells modified with α-linolenic acid, it was found that MDA accumulation rate was relatively slow compared to the other cells and vesicles (Fig. 4d). There was a gradual increase which

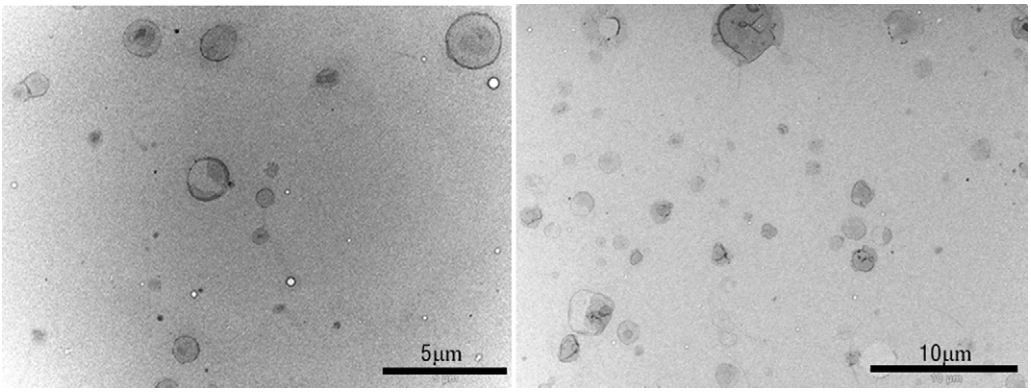

Fig. 3. TEM images of PE–PG lipid vesicles.
Images courtesy of Integrative Biology Microscopy Core Facility, University of South Florida.

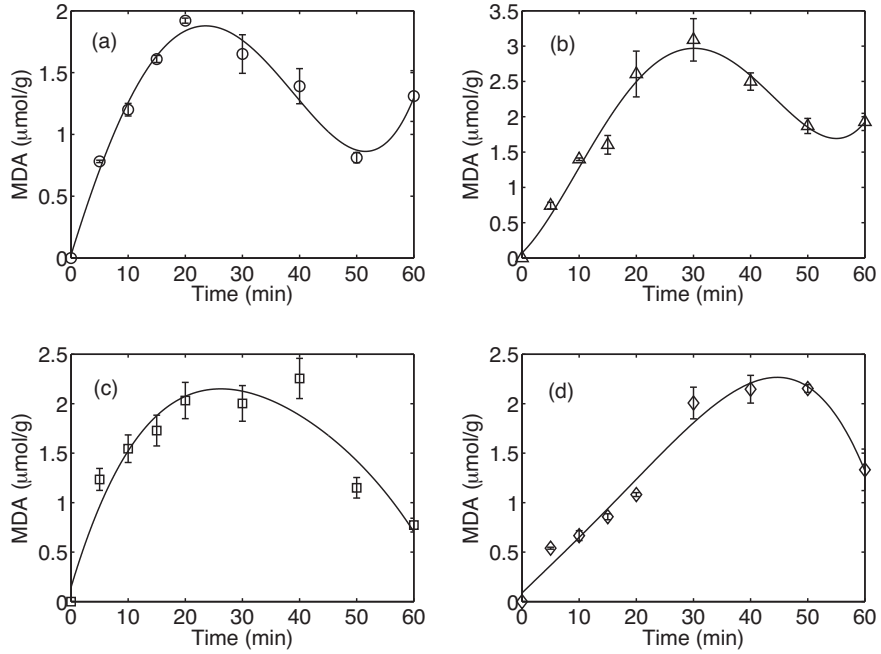

Fig. 4. MDA production during photocatalytic experiments with P25 TiO_2: $I_0 = 4.37 \times 10^{-2} \pm 5.19 \times 10^{-3}$ mE L^{-1} s^{-1}, $C_0 \approx 2.8 \times 10^8$ CFU mL^{-1}: (a) unmodified cells; (b) *E. coli* PE/PG vesicles; (c) cells supplemented with oleic acid; (d) cells supplemented with linolenic acid. The data are fitted with a fourth order polynomial.

peaked around 45 min. Control cells and cells supplemented with oleic acid (C18:1 n-9) did not produce this extended MDA evolution curve, which leads to the belief that the kinetics is affected by the fatty acid composition. However, it is difficult to make a definitive conclusion about the impact of the fatty acid supplementation on MDA production because of the complexity of the system and the undefined sink processes for MDA.

Nonetheless, it is generally expected that increases in polyunsaturated fatty acid content would render the cell more sensitive to oxidation and an increase in the MDA production could be possible. Other studies have shown that the oxidizability of cells can be altered by supplementation with external fatty acids [38–40]. The results in this case seem to suggest that the enriching of the membrane with monounsaturated fatty acids retards the rate of

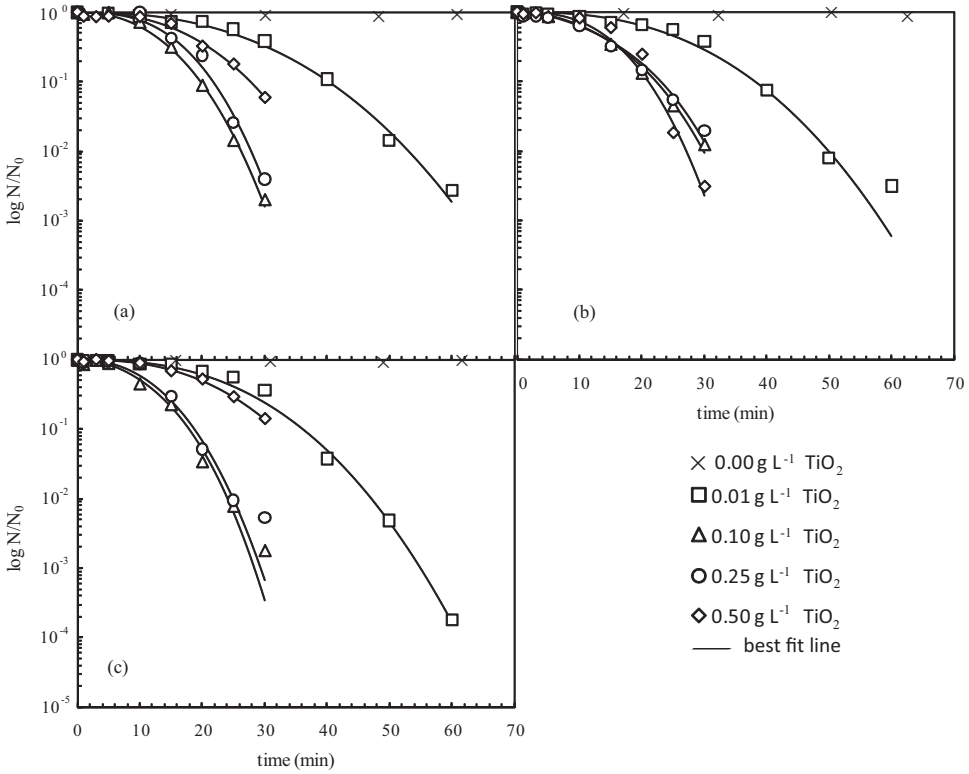

Fig. 5. Survival curves of *E. coli* at low light intensity ($I_0 = 1.35 \times 10^{-2} \pm 2.30 \times 10^{-3}$ mE L^{-1} s^{-1}); (a) cells modified with oleic acid; (b) cells modified with linolenic acid; and (c) control cells (no fatty acid modification).

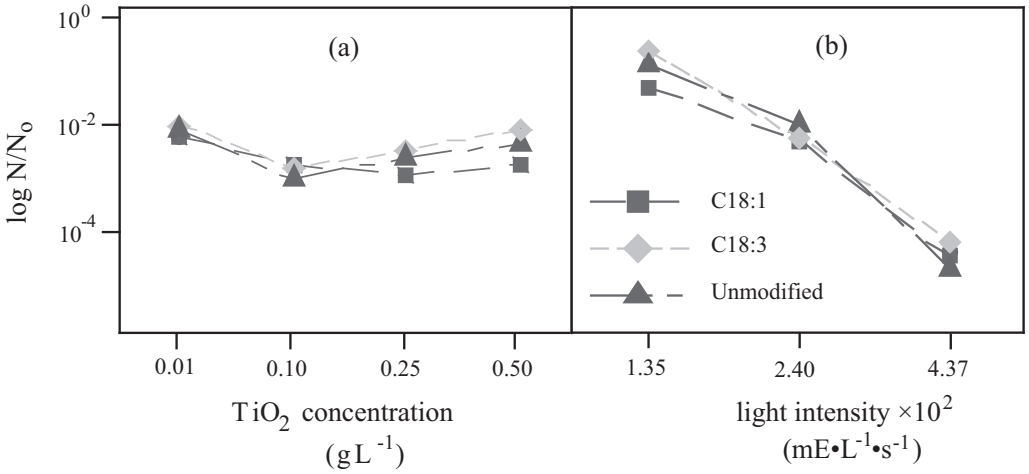

Fig. 6. Effect of fatty acid on overall disinfection at 20 min of exposure: (a) fatty acid modification vs. TiO_2 concentration; and (b) fatty acid modification vs. light intensity.

MDA production, particularly when supplemented with α-linolenic acid. The actual mechanism by which these monosaturated fatty acids are able to reduce the peroxidation rate is still not clear. However, a possible explanation for this observation is the oxidation of monosaturated fatty acids does not produce bioactive byproducts responsible for enhancing membrane peroxidation [39,41]. This effect, described by Lee et al. [39], is similar to an antioxidant in which the monosaturated fatty acids serve as a temporary sink for the capture of free radicals, and retard propagation due to their reduced reactivity.

3.5. Effect of supplemental fatty acid on disinfection

Since there were differences in the time evolution of MDA production during photocatalysis based on fatty acid composition, a series of photocatalytic experiments were conducted to assess whether these differences would translate to disinfection resistance. Instead of using the very high cell concentrations needed to produce measurable MDA in the previous experiments, the cell concentration was lowered to realistic numbers ($C_0 = 1 \times 10^6$ CFU mL^{-1}). In addition, the experiments were conducted at three levels of light intensity ($4.37 \times 10^{-2} \pm 5.19 \times 10^{-3}$, $2.40 \times 10^{-2} \pm 5.19 \times 10^{-3}$, and $1.35 \times 10^{-2} \pm 2.30 \times 10^{-3}$ mE L^{-1} s^{-1}) and varying TiO_2 concentrations (0.01, 0.10, 0.25 and 0.50 g L^{-1}). The survival curves are shown in Fig. 5.

To assess the effect of fatty acid modification on the overall disinfection efficiency, a one-way ANOVA was performed on the survival data from 36 experiments for each modified organism. The analysis revealed that the effect was not statistically significant at the 95% confidence level ($p = 0.071$). Even when the fatty acid modification is analyzed at a specific light intensity values and at different catalyst concentration, there were no significant differences (Fig. 6). Fig. 6 shows the mean survival of the organisms after 20 min of exposure to irradiation in the presence of different loadings of TiO_2 and at different light intensity values. Significant differences were obtained for light intensity ($p = 0.000$) and TiO_2 concentration ($p = 0.002$), but the effect of fatty acid modification was insignificant. Similar results were obtained when the cells were modified with palmitoleic acid (results not shown).

Other researchers [231] working with lipids found that monounsaturated fatty acids tend to retard the progression of peroxidation by acting similar to antioxidants [231]. It is believed that they may react with radicals, but somehow slow their progression and block radical chain reactions. However, the specific explanation for this result is still not yet very clear. Even if the same effect is true in *E. coli*, the effect is not significant in the overall disinfection of the organism for the variation of fatty acids in the study. It indicates that while peroxidation of the cell membrane is a key process during disinfection, small changes in the fatty acid content are not sufficient to cause major changes in the overall disinfection kinetics.

3.6. LOOH production during disinfection

The illumination of TiO_2 in the presence of *E. coli* cells and lipid vesicles yielded measurable concentrations of hydroperoxides (Fig. 6). The nature of the LOOH test ensures that only peroxide generated from the cells is measured. The kit uses a number of internal controls, which correct for endogenous iron content and possible hydrogen peroxide. A significant increase in LOOH concentration was observed during the early stages of the experiments. There was an apparent decrease in the hydroperoxide content at longer illumination times. As in the case of MDA, this trend indicates that the resulting kinetics is a consequence of both photocatalytically induced formation and decomposition of hydroperoxides. This is consistent with the concomitant generation of MDA during the experiments.

These findings are very significant because Fig. 7 shows that the time characteristics for LOOH generation during photocatalytic oxidation of cells and lipid vesicles are very similar. This provides

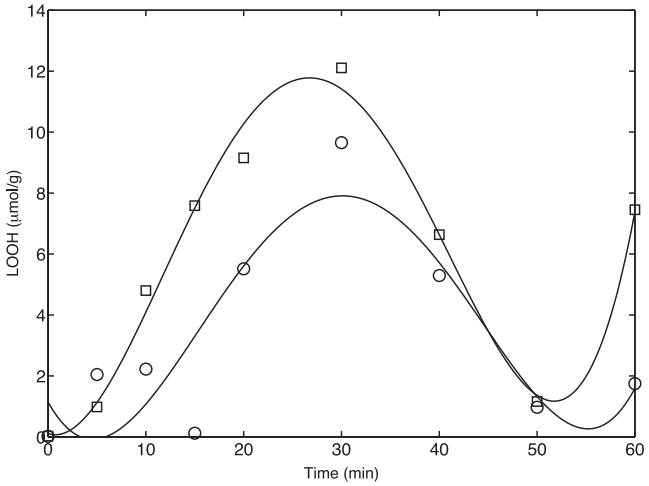

Fig. 7. Time characteristics of lipid hydroperoxide detection during photocatalytic treatment; (○) *E. coli* cells; (□) vesicles prepared with *E. coli* phospholipids.

incontrovertible proof that the cell membrane lipids are the primary targets during photocatalytic inactivation. It also means that lipid vesicles may provide an excellent model system to test the interaction of photocatalysts with cell membranes for disinfection studies in water and medical applications. Lipid vesicles have long been used as models for cellular membranes [41,42], but this is the first reported study that specifically tailored these structures for studies in photocatalytic disinfection studies.

4. Conclusion

The use of lipid vesicles as model membranes provides a suitable alternative to study the peroxidation of cell membranes in photocatalytic studies. By tailoring these structures to be representative of *E. coli* membrane size and composition, useful information to validate peroxidation kinetics has been achieved. It is clear that photocatalytic disinfection for this organism is governed largely by the oxidation of the membrane. This is supported by the fact that the production of both MDA and LOOH during photocatalytic treatment of cells and vesicles show remarkably similar kinetics. However, differences in monounsaturated fatty acids of the cell membrane did not seem to affect the overall disinfection kinetics. The use of this information for the development of a mechanistic model for inactivation may be published elsewhere.

Acknowledgements

This work was supported by the State of Florida through the Florida Energy Systems Consortium (FESC) and the National Science Foundation Research Experience for Undergraduates Grant # 0851910, and in coordination with and the Clean Energy Research Center, University of South Florida.

Appendix A. Supplementary data

Supplementary data associated with this article can be found, in the online version, at doi:10.1016/j.jphotochem.2011.04.025.

References

[1] P. Maness, S. Smolinski, D.M. Blake, Z. Huang, E.J. Wolfrum, W.A. Jacoby, Bactericidal activity of photocatalytic TiO_2 reaction: toward an understanding of its killing mechanism, Appl. Environ. Microbiol. 65 (1999) 4094–4098.
[2] V.A. Nadtochenko, A.G. Rincon, S.E. Stanca, J. Kiwi, Dynamics of *E. coli* membrane cell peroxidation during TiO_2 photocatalysis studied by ATR-FTIR spectroscopy and AFM microscopy, J. Photochem. Photobiol. A 169 (2005) 131–137.
[3] J. Kiwi, V. Nadtochenko, Evidence for the mechanism of photocatalytic degradation of the bacterial wall membrane at the TiO_2 interface by ATR-FTIR and laser kinetic spectroscopy, Langmuir 21 (2005) 4631–4641.
[4] J. Kiwi, V. Nadtochenko, New evidence for TiO_2 photocatalysis during bilayer lipid peroxidation, J. Phys. Chem. B 108 (2004) 17675–17684.
[5] Y.W. Cheng, R.C.Y. Chan, P.K. Wong, Disinfection of *Legionella pneumophila* by photocatalytic oxidation, Water Res. 41 (2007) 842–852.
[6] M.R. Hoffmann, S.T. Martin, W. Choi, D.W. Bahnemann, Environmental applications of semiconductor photocatalysis, Chem. Rev. 95 (1995) 69–96.
[7] R.T. Dean, S. Fu, R. Stocker, M.J. Davies, Biochemistry and pathology of radical-mediated protein oxidation, Biochem. J. 324 (1997) 1–18.
[8] C.L. Hawkins, M.J. Davies, Generation and propagation of radical reactions on proteins, Biochim. Biophys. Acta (BBA)—Bioenerg. 1504 (2001) 196–219.
[9] B.C. Gilbert, D.M. King, C.B. Thomas, The oxidation of some polysaccharides by the hydroxyl radical: An e.s.r. investigation, Carbohydr. Res. 125 (1984) 217–235.
[10] B. Halliwell, J. Gutteridge, Free Radicals in Biology and Medicine, 2nd ed., Clarendon Press, Oxford, 1989.
[11] W.A. Pryor (Ed.), Free Radicals in Biology, Academic Press, Inc., New York, 1976.
[12] H.W. Gardner, Oxygen radical chemistry of polyunsaturated fatty acids, Free Radic. Biol. Med. 7 (1989) 65–86.
[13] J.A. Imlay, S. Linn, DNA damage and oxygen radical toxicity, Science 240 (1988) 1302–1309.
[14] G. Gogniat, S. Dukan, TiO_2 photocatalysis causes DNA damage via Fenton reaction-generated hydroxyl radicals during the recovery period, Appl. Environ. Microbiol. 73 (2007) 7740–7743.
[15] O.K. Dalrymple, E. Stefanakos, M.A. Trotz, D.Y. Goswami, A review of the mechanisms and modeling of photocatalytic disinfection, Appl. Catal. B 98 (2010) 27–38.
[16] B. Halliwell, S. Chirico, Lipid peroxidation: its mechanism, measurement, and significance, Am. J. Clin. Nutr. 57 (1993) 715S–724S.
[17] J.E Cronan Jr, Phospholipid alterations during growth of *Escherichia coli*, J. Bacteriol. 95 (1968) 2054–2061.
[18] M. Kito, S. Aibara, M. Kato, T. Hata, Differences in fatty acid composition among phosphatidylethanolamine, phosphatidylglycerol and cardiolipin of *Escherichia coli*, Biochim. Biophys. Acta (BBA)—Lipids Lipid Metab. 260 (1972) 475–478.
[19] W.M Oleary, Fatty acids of bacteria, Bacteriol. Rev. 26 (1962) 421.
[20] A.G. Marr, J.L. Ingraham, Effect of temperature on the composition of fatty acids in *Escherichia coli*, J. Bacteriol. 84 (1962) 1260–1267.
[21] C.O. Gill, J.R. Suisted, The effects of temperature and growth rate on the proportion of unsaturated fatty acids in bacterial lipids, J. Gen. Microbiol. 104 (1978) 31–36.
[22] K. Magnuson, S. Jackowski, C.O. Rock, J.E. Cronan Jr, Regulation of fatty acid biosynthesis in *Escherichia coli*, Microbiol. Mol. Biol. Rev. 57 (1993) 522–542.
[23] M.A. Cubillos, E.A. Lissi, E.B. Abuin, Kinetics of lipid peroxidation in compartmentalized systems initiated by a water-soluble free radical source, Chem. Phys. Lipids 104 (2000) 49–56.
[24] P.R. Cullis, B. De Kruijff, The polymorphic phase behaviour of phosphatidylethanolamines of natural and synthetic origin. A 31P NMR study, Biochim. Biophys. Acta (BBA)—Biomembr. 513 (1978) 31–42.
[25] P.L. Yeagle, A. Sen, Hydration and the lamellar to hexagonal(II) phase transition of phosphatidylethanolamine, Biochemistry 25 (1986) 7518–7522.
[26] N.J. Bunce, J. LaMarre, S.P. Vaish, Photorearrangement of azoxybenzene to 2-hydroxyazobenzene: a convenient chemical actinometer, Photochem. Photobiol. 39 (1984) 531–533.
[27] Z.-Y. Jiang, A. Woollard, S. Wolff, Lipid hydroperoxide measurement by oxidation of Fe_2^+ in the presence of xylenol orange. Comparison with the TBA assay and an iodometric method, Lipids 26 (1991) 853–856.
[28] Z.-Y. Jiang, J.V. Hunt, S.P. Wolff, Ferrous ion oxidation in the presence of xylenol orange for detection of lipid hydroperoxide in low density lipoprotein, Anal. Biochem. 202 (1992) 384–389.
[29] J.E. Cronan Jr., C.O. Rock, The presence of linoleic acid in *Escherichia coli* cannot be confirmed, J. Bacteriol. 176 (1994) 3069–3071.
[30] M.T. Magdigan, J.M. Martinko, Brock Biology of Microorganisms, 11th ed., Pearson Education, Inc., Upper Saddle River, NJ, 2006.
[31] D.R. Janero, Malondialdehyde and thiobarbituric acid-reactivity as diagnostic indices of lipid peroxidation and peroxidative tissue injury, Free Radic. Biol. Med. 9 (1990) 515–540.
[32] A.M. Jentzsch, H. Bachmann, P. Fürst, H.K. Biesalski, Improved analysis of malondialdehyde in human body fluids, Free Radic. Biol. Med. 20 (1996) 251–256.
[33] J.M.C. Gutteridge, The use of standards for malonyldialdehyde, Anal. Biochem. 69 (1975) 518–526.
[34] K.J. Dennis, T. Shibamoto, Gas chromatographic determination of malonaldehyde formed by lipid peroxidation, Free Radic. Biol. Med. 7 (1989) 187–192.
[35] K. Moore, L.J. Roberts, Measurement of lipid peroxidation, Free Radic. Res. 28 (1998) 659–671.
[36] Q.-T. Li, M.H. Yeo, B.K. Tan, Lipid peroxidation in small and large phospholipid unilamellar vesicles induced by water-soluble free radical sources, Biochem. Biophys. Res. Commun. 273 (2000) 72–76.
[37] A.F. Vikbjerg, T.L. Andresen, K. Jørgensen, H. Mu, X. Xu, Oxidative stability of liposomes composed of docosahexaenoic acid-containing phospholipids, J. Am. Oil Chem. Soc. 84 (2007) 631–637.
[38] C.M. Hart, J.K. Tolson, E.R. Block, Supplemental fatty acids alter lipid peroxidation and oxidant injury in endothelial cells, Am. J. Physiol. Lung Cell. Mol. Physiol. 260 (1991) L481–L488.
[39] C. Lee, J. Barnett, P.D. Reaven, Liposomes enriched in oleic acid are less susceptible to oxidation and have less proinflammatory activity when exposed to oxidizing conditions, J. Lipid Res. 39 (1998) 1239–1247.
[40] B.A. Wagner, G.R. Buettner, C.P. Burns, Free radical-mediated lipid peroxidation in cells: oxidizability is a function of cell lipid bis-allylic hydrogen content, Biochemistry 33 (2002) 4449–4453.
[41] S.N. Chatterjee, S. Agarwal, Liposomes as membrane model for study of lipid peroxidation, Free Radic. Biol. Med. 4 (1988) 51–72.
[42] L.R.C. Barclay, Models biomembranes: quantitative studies of peroxidation, antioxidant action, partitioning, and oxidative stress, Can. J. Chem. 71 (1993) 1–16.